A Role for SNAP25 in Internalization of Kainate Receptors and Synaptic Plasticity

Sanja Selak,[1,2] Ana V. Paternain,[1,2] Isabel M. Aller,[1] Esther Picó,[1] Rocio Rivera,[1] and Juan Lerma[1,*]
[1]Instituto de Neurociencias de Alicante, CSIC-UMH, 03550 San Juan de Alicante, Spain
[2]These authors contributed equally to this work
*Correspondence: jlerma@umh.es
DOI 10.1016/j.neuron.2009.07.017

SUMMARY

Regulation of surface insertion and internalization of AMPA and NMDA receptors has emerged as a key mechanism for the control of synaptic strength. Regulatory elements for synaptic kainate receptors (KARs) are, however, largely undetermined. We have found that SNAP25 is critical for the synaptic removal of KARs, acting via GluK5 (i.e., KA2) subunits. SNAP25 coimmunoprecipitates with protein complexes containing PICK1, GRIP1, and GluK5 and colocalizes with GluK5 in both hippocampal neurons and transfected HEK293 cells. In hippocampal slices, purified SNAP25 antibodies and blocking peptides caused a GluK5-dependent run-up of KARs-mediated EPSC (EPSC$_{KAR}$) recorded from CA3 pyramidal neurons when included in the patch pipette and prevented activity-dependent long-term depression of EPSC$_{KAR}$. As EPSC$_{KAR}$ LTD, SNAP25/PICK1/GluK5 interactions are dynamically regulated by PKC.

INTRODUCTION

An essential aspect for neurotransmitter receptors function is the appropriate localization and cell surface expression in neurons. Indeed, differential subunit trafficking, targeting, and selective assembly tightly regulates the diverse physiological roles of glutamate receptors, and these events are controlled through interactions with proteins that bind to cytoplasmic domains on the specific receptor subunits. Glutamate is the major excitatory neurotransmitter in the mammalian brain, and it activates three types of ionotropic receptors: NMDA, AMPA, and kainate. However, our understanding of mechanisms that regulate KAR trafficking lags far behind that for other receptors, and only lately has it begun to grow. KARs modulate synaptic transmission and neuronal excitability by acting at presynaptic, postsynaptic, or extrasynaptic sites (Huettner, 2003; Lerma, 2003). KARs are assembled by five different subunits: GluK1-GluK3, GluK4, and GluK5. [In this paper, we are adopting the new nomenclature for KARs, recently recommended by the IUPHAR, where GluR5, GluR6, GluR7, KA1, and KA2 correspond to GluK1, GluK2, GluK3, GluK4, and GluK5, respectively (see Collingridge et al., 2009).] GluK1-3 can coassemble as homomers or hetero-mers with each other, giving rise to functional receptors (Cui and Mayer, 1999; Paternain et al., 2000), whereas GluK4 and GluK5 must coassemble with at least one subunit from GluK1-3 to form functional receptors.

Since KAR subunits differ in their C-terminal domains, their differential trafficking is likely attributable to interactions with distinct subsets of cytoplasmic trafficking proteins (Coussen et al., 2005). Although GluK1-4 subunit-mediated regulation of KAR function has been explored in recent studies, much less is known about the signaling pathways that regulate GluK4 and GluK5 function via the proteins interacting with their C termini. Several PDZ domain-containing proteins, PSD-95, PICK1, GRIP, and syntenin, were shown to interact with the extreme C termini of GluK2 and two splice variants of GluK1 (GluK1b and GluK1c) (Garcia et al., 1998; Hirbec et al., 2003). Interestingly, PICK1 and GRIP have been previously identified as proteins also interacting with the AMPA receptor subunit GluA2 (Hirbec et al., 2003; Xia et al., 1999).

GluK5 subunits are key elements of synaptic responses, as it has been clearly illustrated at the level of mossy fibers to CA3 contacts. Unlike other KAR subunits, the GluK5 subunit contains a unique and much longer C terminus (150 aa), which contains specific endoplasmic reticulum (ER) retention and forward trafficking motifs allowing selective plasma membrane targeting (Ren et al., 2003; Jaskolski et al., 2004). GluK5 also contains a C-terminal dileucine endocytic motif that is highly selective for clathrin internalization pathways (Ren et al., 2003).We reasoned that the GluK5 subunit might engage additional and differential protein interactions that might specifically regulate the function of heteromeric GluK5-containing KARs. Therefore, we set out to determine if the function of GluK5 subunit is regulated by the proteins that were previously implicated in GluR subunit trafficking and to identify additional GluK5-binding partners. Here, we report regulation of GluK5 subunit-containing KARs by interactions involving SNAP25 and PICK1. Blockade of SNAP25 function during recording of CA3 neurons lead to an increase of KAR-mediated EPSCs, and the cells overexpressing SNAP25 were characterized by an increased intracellular accumulation of GluK5-containing receptors. Postsynaptic long-term depression (LTD) of KAR-mediated EPSC was prevented by disrupting the interaction between SNAP25 and GluK5. Our data indicate that SNAP25 interactions with GluK5 and PICK1 reduce the GluK5 stability on the membrane, favoring or facilitating KAR internalization. These data establish an unexpected role of SNAP25 in regulation of glutamate receptor trafficking and activity-dependent plasticity of a synaptic component mediated by KARs.

RESULTS

Interaction of SNAP25, GRIP, and PICK1 with GluK5 Subunits

To identify the protein complexes associated with GluK5 subunits in the central nervous system, we performed coimmunoprecipitations from membrane fractions of hippocampal homogenate prepared from C57/Bl6 wild-type or $GluK5^{-/-}$ mice (used as a control for the precipitating antibody). GluK5 protein was immunoprecipitated using two well-characterized affinity-purified anti-GluK5 antibodies recognizing either the last 8 (C8) (Herb et al., 1992) or the last 20 amino acids of the GluK5 C terminus (C20) (Darstein et al., 2003). Western blots were performed using antibodies against the proteins previously implicated in the modulation of KAR function. In the course of these experiments, we unexpectedly discovered that SNAP25 was associated with GluK5 in biochemically isolated complexes. As shown in Figure 1, SNAP25 and GRIP coimmunoprecipitated with GluK5 protein from wild-type (Figure 1A) but not from $GluK5^{-/-}$ hippocampi (Figure 1B), indicating the specificity of the immunoprecipitation. To control for the specificity of GluK5:SNAP25 interaction, we tested the presence of either syntaxin1 (t-SNARE) or VAMP2/synaptobrevin (v-SNARE), both of which are present in nerve terminals as parts of the presynaptic SNARE complexes together with SNAP25 (Baumert et al., 1989; Söllner et al., 1993). Neither syntaxin1 nor VAMP-2/synaptobrevin was detected in the GluK5 immunoprecipitates (Figure 1A). Since SNAP25 has been shown to bind endosomal proteins and so mediate the fusion of endosomal vesicles (Sun et al., 2003; Yan et al., 2004), we also tested whether the endosomal SNAP25 fusion partners such as Hepatocyte growth factor/HGF-receptor substrate (Hrs) were present in the GluK5 antibody precipitates. Hrs was precipitated neither with GluK5 nor with PICK1 or GRIP antibody (data not shown). To verify the successful immunoprecipitation of GluK5 subunit, blots were stripped and reprobed with anti-GluK5 antibody, and as expected, immunoreactivity was detected only in wild-type and not in the samples from $GluK5^{-/-}$ mice. Since only a small amount of SNAP25 was pulled down by this approach, to further investigate the specificity of this binding, we performed a reciprocal coimmunoprecipitation using a monoclonal antibody to SNAP25 protein. To reduce the dissociation of the antibodies from the beads during the elution of IP complexes, we covalently coupled equal amounts of anti-SNAP25 antibody and a normal mouse immunoglobulin G (IgG), which was used as a control. In the protein complexes pulled down with the SNAP25 antibody but not with control mouse IgG, we detected coimmunoprecipitation of GluK5 and GRIP and a robust signal for PICK1 (Figure 1C). Such apparent interaction with PICK1 uncovered by SNAP25 antibodies lead us to think that PICK1 could be present in GluK5-associated complexes and that it was not immunoprecipitated by GluK5 antibodies due to the limitations associated with the use of the C-terminal anti-GluK5 antibody. Indeed, native GluK5 receptors were precipitated with polyclonal anti-GluK5 antibodies raised against a peptide mapping to the last 8 or 20 amino acids of the GluK5 C terminus. Therefore, some protein interactions may not be detected using these antibodies because of interference between the antibody and interacting

protein binding site. Indeed, PICK1 binding motifs are located at the four terminal amino acids of the AMPA and KA receptors (Hirbec et al., 2003; Xia et al., 1999). To overcome this problem, we carried out pull-down experiments using the GluK5 C-terminal domain fused to GST. In these experiments, native PICK1 and SNAP25 were efficiently retained by GST-GluK5$_{C\text{-term}}$ but not by GST alone, particularly if suitable conditions for protein phosphorylation were established (e.g., in the presence of ATP-Mg^{2+}) (Figure 1D).

The specificity of SNAP25 coIP with GluK5 was additionally tested by immunoprecipitation of GluK5 using a covalently coupled rabbit anti-GluK5 antibody (C8), to prevent the elution of immunoglobulins and so facilitate the detection of pulled down proteins by western blot (see Figure S2). Using this approach, we precipitated a greater amount of SNAP25 in a complex with GluK5 in both synaptic (LP1) and light, nonsynaptic (P3) membrane fractions. These results indicate that SNAP25 and GluK5 protein complexes exist at both synaptic and nonsynaptic sites.

To investigate whether SNAP25 interaction with GluK5 can be isolated in a reduced experimental system, we used HEK293 cells, which do not express either SNAP25 or GluK5 but express GRIP and PICK1 (Figure S1). We transfected HEK293 cells with either N-terminal-tagged EGFP-SNAP25 or a control EGFP vector along with N-terminal myc-tagged GluK5 and untagged GluK1$_{2a}$ subunit (to allow targeting of GluK5 receptors to the membrane). The GluK1$_{2a}$ subunit was chosen because it is a GluR subunit containing the shortest C terminus (16 aa) that does not engage in the interactions with any of the known KAR-interacting proteins (Hirbec et al., 2003). EGFP-SNAP25 labeled the periphery of cells when expressed alone (data not shown). Furthermore, colocalization studies using anti-GluK5 antibody (C20) indicated that myc-GluK5 and EGFP-SNAP25, but not EGFP vector alone, colocalized on the plasma membrane of the triply transfected cells (Figure S1), demonstrating that GluK5 and SNAP25 could interact at this compartment. Consistently, we detected a weak but demonstrable coimmunoprecipitation of EGFP-SNAP25 with GluK5 subunits in these cells, a result that was reproducible in three independent experiments (Figure S1). The weak EGFP-SNAP25 binding to myc-GluK5 can be explained, at least in part, by the fact that not all cells that were transfected with myc-GluK5 were coexpressing EGFP-SNAP25 constructs.

These biochemical approaches indicate that interaction of SNAP25 and GluK5 appears rather weak. This fact could be derived from a rather transient and/or dynamic functional interaction of SNAP25 and GluK5. Then, we asked whether bimolecular fluorescence complementation (BiFC) (Kerppola, 2006) might provide an approach to demonstrate this interaction in vivo. BiFC takes advantage of the fact that when the two nonfluorescent amino- and carboxy-terminal fragments of yellow fluorescent protein (YFP) are brought into close apposition they interact, leading to the irreversible formation of a fluorescent protein, and could reveal the formation of protein complexes even if only a fraction of each protein interacts (Saka et al., 2007). To that end, we have used an optimized version of the YFP variant Venus (Saka et al., 2007). Fusion proteins were generated fusing the N-terminal domain (V154m9) of Venus to GluK5 (GluK5^{VNT}) and
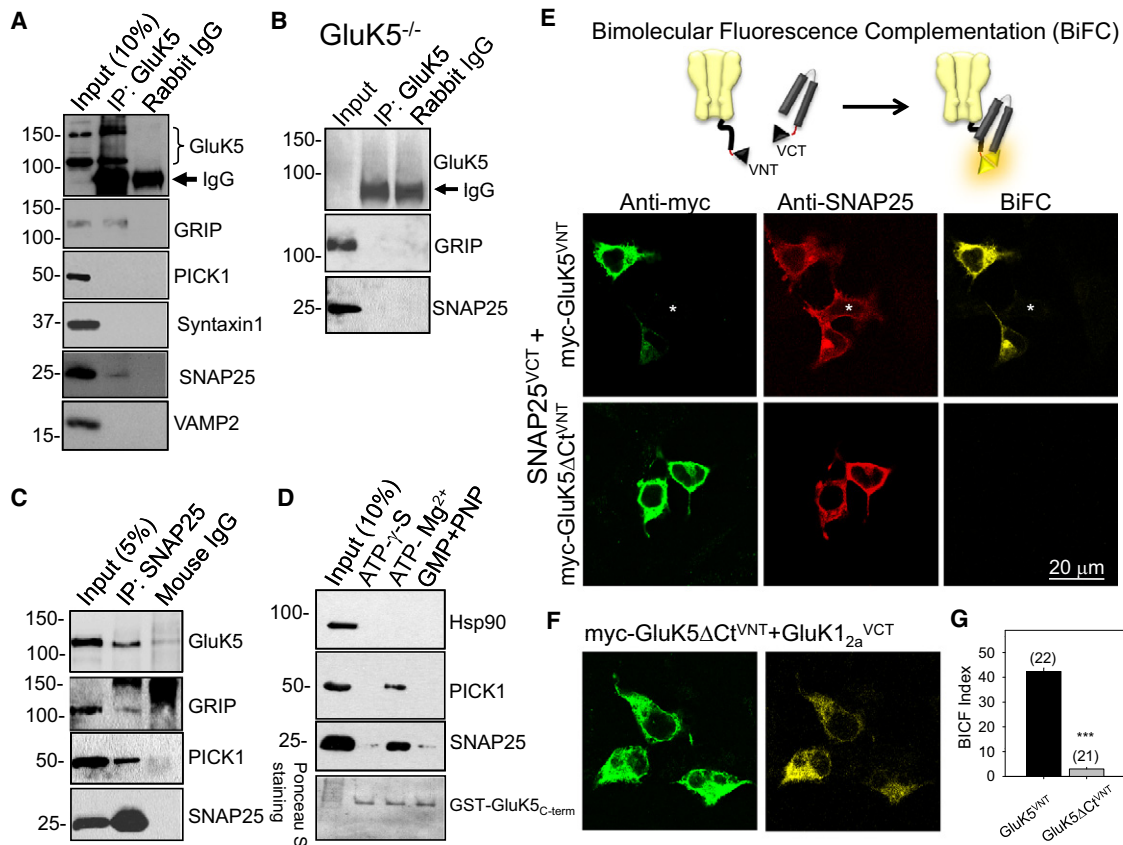
Figure 1. GluK5 Kainate Receptor Subunits Coimmunoprecipitate with SNAP25

Hippocampus homogenate from C57 WT (A) or $GluK5^{-/-}$ (B) mice was used for immunoprecipitation with anti-GluK5 antibody. GRIP and SNAP25, but neither presynaptic exocytic SNARE proteins (syntaxin1, VAMP2) nor the endosomal SNAP25 fusion partner Hrs coimmunoprecipitated with GluK5 subunits from WT hippocampus homogenate. PICK1 was not detected in the GluK5-containing complexes using this approach.

(B) Control coimmunoprecipitation from $GluK5^{-/-}$ hippocampus homogenate with anti-GluK5 antibody. GRIP and SNAP25 were not coimmunoprecipitated with anti-GluK5 antibody in the absence of GluK5 protein.

(C) SNAP25 coimmunoprecipitated GluK5, GRIP and PICK1 from mouse hippocampus homogenate.

(D) SNAP25 and PICK1 bind to C terminus of GluK5 under ATP hydrolysis conditions. GST-tagged GluK5 C-terminal deletion mutant or GST tag alone were bound to glutathione sepharose beads and incubated with mouse brain homogenate in the nucleotide buffer containing either 2 mM EDTA and 1 mM nonhydrolysable ATP homolog or in the presence of 2 mM $MgCl_2$ and 1 mM ATP.

(E) Demonstration of SNAP25-GluK5 interaction by bimolecular fluorescence complementation (BiFC). BiFC takes advantage of the fact that when the two nonfluorescent amino- and carboxy-terminal fragments of yellow fluorescent protein (YFP) are brought into close apposition they interact leaving to the irreversible formation of a fluorescent protein. HEK cells were cotransfected with GluK5 and SNAP25 fusion proteins to which the N-terminal (VNT) and C-terminal (VCT) domains of the YFP variant Venus had been added (cartoon) as well as with $GluK5_{2a}$ to allow GluK5 exit from ER. Double immunolabeling, using antibodies against myc (Alexa 555; green) and SNAP25 (Alexa 647, red), was also performed to check for the levels of protein expression. Single confocal images showing that cotransfection of $GluK5^{VNT}$ and $SNAP25^{VCT}$ leads to the reconstitution of Venus in those cells where both proteins are expressed (top row). Removal of the C-terminal domain of GluK5 (myc-GluK5ΔC^{VNT}) selectively prevents fluorescence complementation (lower row).

(F) As a control, the viability of myc-GluK5ΔC^{VNT} was assessed by its cotransfection with GluK1$_{2a}$ fused to the C-terminal domain of Venus (GluK1$_{2a}^{VCT}$). Heteromerization of these subunits to form a heteromeric kainate receptor produces fluorescence complementation (righthand panel).

(G) Degree of fluorescence complementation (BiFC) obtained for $SNAP25^{VCT}$ cotransfected with either myc-GluK5^{VNT} (black bar) or GluK5ΔCT^{VNT} deletion mutant (gray bar). An arbitrary BiFC index was calculated as the yellow fluorescence normalized to the sum of green (myc) and red (SNAP25) fluorescence measured in each cell. Indicated numbers are the cells analyzed from three independent experiments. ***$p < 0.001$, Student's t test.

Bars are means ± SEM; ***$p < 0.001$, Student's t test.

the C-terminal domain (V155) of Venus to SNAP25 ($SNAP25^{VCT}$). Figure 1E shows the results of these experiments. Cotransfection of $GluK5^{VNT}$ and $SNAP25^{VCT}$ led to the reconstitution of Venus in those cells where both proteins were expressed (Figure 1E). To demonstrate the presence of SNAP25 and GluK5 in the same cell, we subjected the cells to double immunolabeling, using antibodies against myc and SNAP25. Interestingly, removal of the

C-terminal domain of GluK5 (myc-GluK5ΔC^{VNT}) selectively prevented fluorescence complementation (Figures 1E and 1G), although immunocytochemical analysis demonstrated normal levels and subcellular localization of expressed proteins. As a further control, the viability of myc-GluK5ΔC^{VNT} was assessed by its cotransfection with GluK1$_{2a}$ fused to the C-terminal domain of Venus (GluK1$_{2a}^{VCT}$). Heteromerization of these subunits to
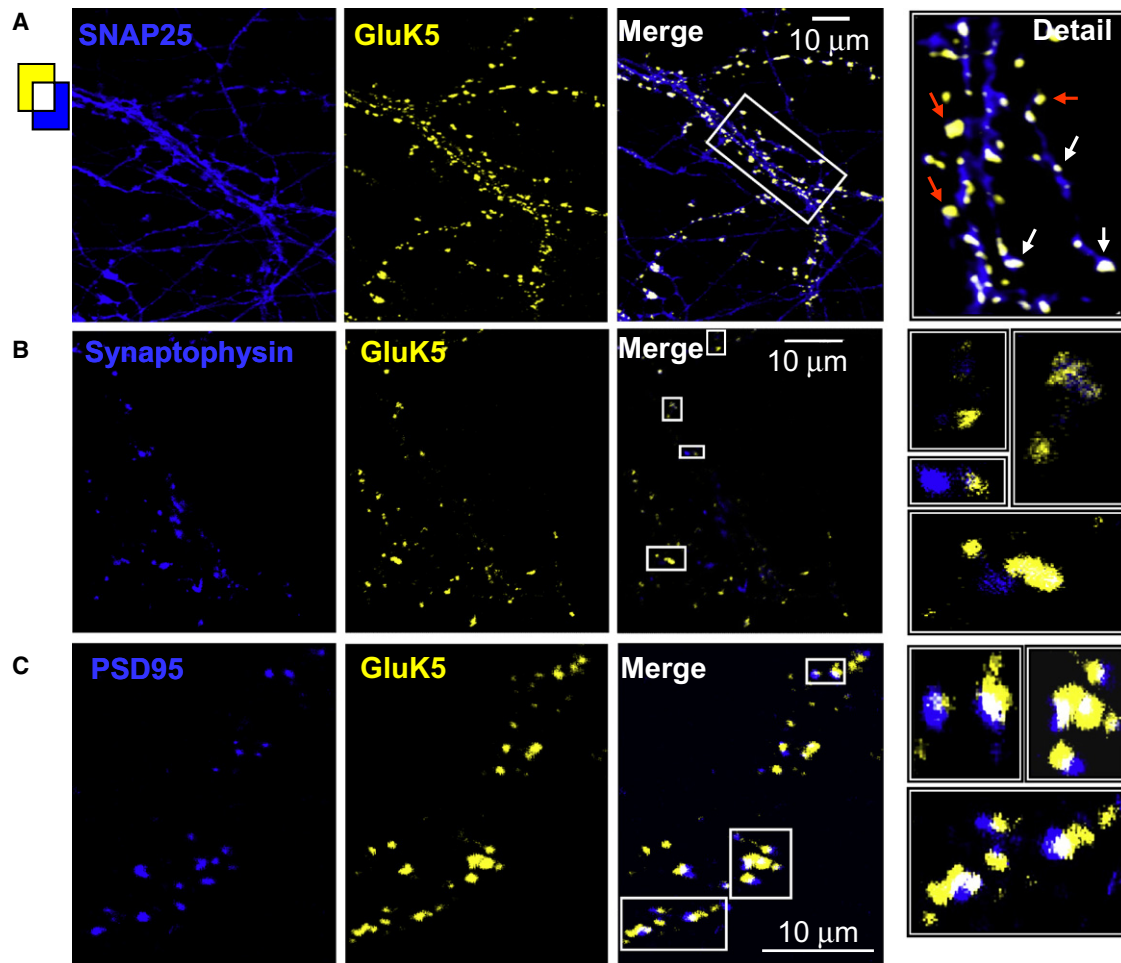
Figure 2. GluK5 and SNAP25 Colocalize in the Postsynaptic Compartments of the Hippocampal Neurons
(A) In DIV26 hippocampal neurons, SNAP25 (blue) and GluK5 (yellow) colocalized in the ~50% of immunolabeled puncta.
(B) Immunolocalization of synaptophysin (blue) and GluK5 (yellow) indicates that GluK5 is in close proximity but clearly separated from the presynaptic, synaptophysin-labeled compartments (inserts show magnification of the selected regions).
(C) PSD95 (blue) and GluK5 (yellow) colocalized in ~50% of puncta. GluK5 label is also detected in extrasynaptic compartments.

form a heteromeric kainate receptor produced fluorescence complementation (Figure 1F), excluding unviability of GluK5 deletion mutant as the reason for the absence of complementation in the previous experiment. These results strongly support the idea that complementation of the wild-type proteins reflects a specific interaction and, although fluorescence complementation does not establish that fusion proteins interact directly, they further strengthen that GluK5 and SNAP25 take part of the same complex in the living cell.

Taken together, our data identify SNAP25 as a GluK5 subunit interacting partner in both native and recombinant systems and fairly indicate that GluK5 subunits form a complex with SNAP25, PICK1 and GRIP proteins.

SNAP25 and GluK5 Colocalize in the Postsynaptic Compartments of Mouse Hippocampal Neurons
GluK4 and GluK5 subunits are present in the presynaptic boutons and vesicular structures, but they are predominantly post-

synaptic (Darstein et al., 2003). SNAP25 functions as a SNARE protein that regulates synaptic vesicle exocytosis at presynaptic nerve terminals. However, SNAP25 expression is not limited to the presynaptic compartments (Tao-Cheng et al., 2000). Therefore, it was important to determine in which neuronal compartment SNAP25 and GluK5 colocalize. In cultured hippocampal neurons, GluK5 label was detected as distinct puncta distributed along the plasma membrane, many of which colocalized with SNAP25 label (Figure 2A). However, GluK5 did not colocalize with synaptophysin, a protein present exclusively in the presynaptic terminals (Wiedenmann and Franke, 1985; Rehm et al., 1986) (Figure 2B). Careful examination of the individual nerve terminals indicated that GluK5 and synaptophysin antibodies label the structures sometimes closely opposed to each other but never overlapping (Figure 2B, insets). In contrast, ~50% of GluK5 puncta colocalized with PSD95 (Figure 2C), a protein associated with the postsynaptic membrane (e.g., Sampedro et al., 1981). These data demonstrate that in these
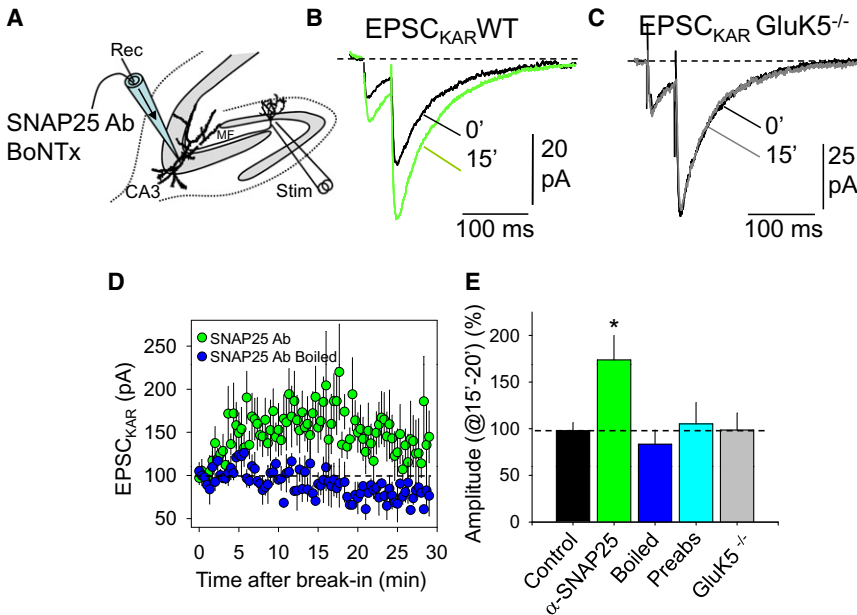
Figure 3. Interfering with SNAP25 Postsyn-aptically Produces a Run-Up of Kainate Receptor-Mediated EPSCs (EPSC_KAR), Recorded from CA3 Pyramidal Neurons under Whole-Cell Configuration

Mossy fiber activation was achieved by stimulating dentate gyrus.

(A) A diagram with the arrangement of recording patch pipette and stimulating electrode.

(B) Dialysis of SNAP25 purified antibodies from the whole-cell recording pipette caused a progressive increase in the size of EPSCs mediated by KARs recorded from WT but not from $GluK5^{-/-}$ mice.

(C). The examples correspond to averages of four responses collected at the indicated time points.

(D) Time course of EPSC amplitude variation mediated by KARs when the intact (green symbols) or boiled (blue symbols) SNAP25 antibody was included in the patch pipette internal solution.

(E) Summary of the effects of different treatments on KAR-mediated EPSC. The action of SNAP25 antibodies was specific for KARs containing GluK5 subunits.

Bars are means ± SEM; *$p < 0.05$, Student's t test.

cultured hippocampal neurons GluK5 is expressed in the soma-todendritic and postsynaptic compartments and indicate that the observed colocalization of GluK5 and SNAP25 does not include presynaptic nerve terminals, at least to a significant degree.

Functional Blockade of SNAP25 Increases KAR-Mediated EPSCs in CA3 Hippocampal Neurons

Since SNAP25 colocalized with GluK5 at the postsynaptic sites and it also coimmunoprecipitated with GluK5 and the KAR-interacting protein PICK1, we questioned whether SNAP25 function may be important for KAR activity. Synapses established by mossy fibers onto CA3 dendrites show a KAR-driven current component, which is mediated by GluK5/GluK2 heteromeric receptors (Contractor et al., 2003; Mulle et al., 1998). Therefore, we performed electrophysiological recordings from CA3 neurons, including in the recording pipette protein G-purified mouse monoclonal SNAP25 immunoglobulin (IgG) (Figure 3A) (see Figure S3). Given the small amplitude of KAR-mediated EPSC (EPSC_KAR), we applied two electric pulses to facilitate measurement. When purified anti-SNAP25 antibody was included in the recording solution (20 µg/ml), the KAR-mediated EPSC progressively increased in size (Figures 3B and 3D), reaching a value of 174% ± 26% of control (n = 10; p < 0.05), which was significantly higher than the value obtained in the absence of antibodies (97.9% ± 8.7%; n = 6). The specificity of the anti-SNAP25 antibody effects was additionally demonstrated by either including in the pipette denatured anti-SNAP25 antibody or the antibody preadsorbed against SNAP25 antigen (see also Figure S4). No increase in EPSC_KAR was observed in either case within 30 min after break-in (83.5% ± 17.6%, n = 3, and 105.1% ± 22.8%, n = 6, respectively). The specificity of SNAP25 on KAR function was further assessed by probing SNAP25 antibodies in mice lacking GluK5 subunits. These mice have normal transmission at mossy fiber to CA3 synapses,

albeit the lack of GluK5 subunits makes synaptic responses to decay faster (Contractor et al., 2003) (compare Figures 3B and 3C). In these mice, SNAP25 antibody had no action (98.6% ± 18.3%, n = 7), indicating the requirement for GluK5 subunits of kainate receptors to interact with SNAP25. We also quantified the paired-pulse facilitation (PPF; the ratio of the second over the first EPSC_KAR) as a form of assessing any change in the release properties. PPF remained constant over the recording period (3.9 ± 0.21 versus 4.2 ± 0.42), indicating that transmitter release was not affected during these experiments.

There is no clear evidence linking SNAP-25 to endocytosis or destabilization of receptor complexes. Therefore, we wondered whether these effects are specific to SNAP-25 function as a SNARE protein. To address this question, we performed experiments using light chains of clostridial toxins that specifically cleave SNARE motifs of different SNAREs. If, as indicated by the above results the activity of SNAP25 is related to internalization of KARs, then botulin toxin (BoNT)-A treatment should cause an increase in KAR-mediated responses and should mimic the effect of SNAP25 antibodies. Thus, KAR-mediated EPSC was evaluated during recordings that included the light chain of clostridial toxins in the patch pipette. We found that BoNT-A (1 µM), that cleaves off the nine amino acids at the C-terminal motif of SNAP25, produced a run-up of synaptic responses (157.4% ± 15.5%; n = 9: p < 0.05) (Figure 4A). It was also important to see if cleaving other SNAREs would also lead to a similar rise in KAR-mediated synaptic responses. Then we assayed tetanus toxin (TeTx, 0.1 µM), which cleaves the SNARE protein VAMP-2/synaptobrevin (e.g., Schiavo et al., 2000). Surprisingly, this toxin produced no significant changes in the amplitude of KAR-mediated synaptic responses (109.1% ± 2.4%; n = 7). Activity of TeTx on VAMP-2 cleavage was tested by incubating brain homogenates with the toxin and western blotting. The density of VAMP-2 band was reduced to more than 50% of the control, while SNAP25 band remained unchanged (Figure 4B,
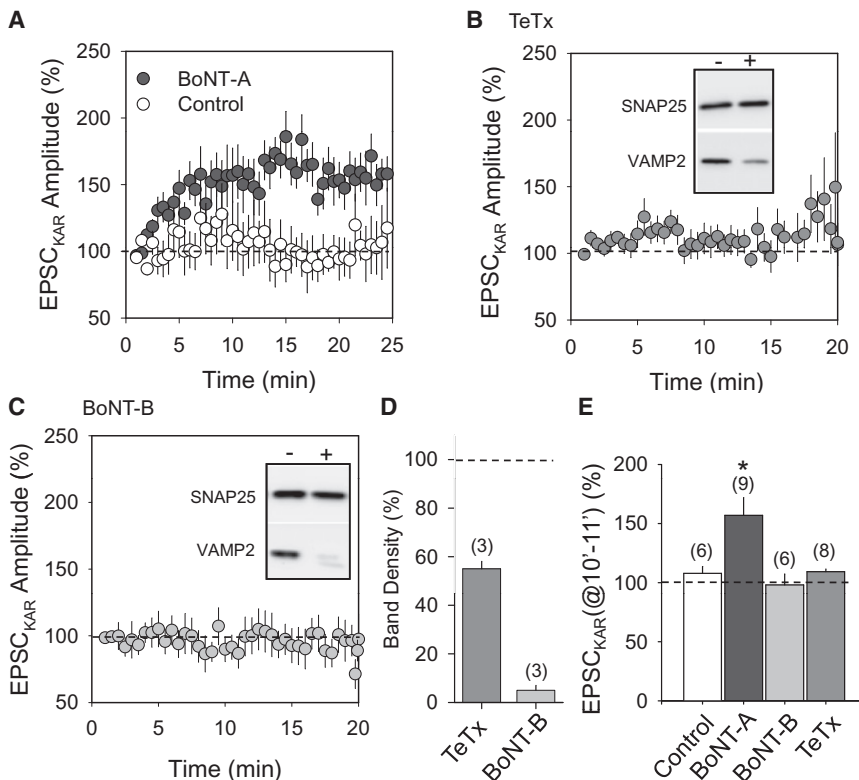
Figure 4. Effect of Clostridial Toxins on KAR-Mediated EPSC

Panels show the time course of KAR-mediated EPSC amplitude when the light chains of clostridial neurotoxins Botulin A (1μM; BoNT-A) (A), Tetanus Toxin (TeTx; 0.1 μM) (B), or Botulin B (BoNT-B, 0.5 μM) (C) were included in the patch pipette. Control (open symbols in A) corresponds to inter-leaved recordings without toxin added. The insets are western blots demonstrating that the TeTx and BoNt-B were active at the used concentrations. (D) Degree of reduction in VAMP-2 band density in toxin-treated samples as compared to untreated samples (n = 3). (E) Only BoNT-A induced a significant increase in the size of CA3 synaptic responses. The number of neurons is indicated in parenthesis in each case. All measurements are expressed as the mean ± SEM, *p < 0.05, two-tailed Student's t test.

inset). To further exclude a role of VAMP-2 in SNAP-25 action, we used BoNT-B (0.5 μM) and although it efficiently cleaved VAMP-2 (>90%; Figure 4C, inset), had no action on the amplitude of EPSC$_{KAR}$ (98.1% ± 9.3%, n = 8, after 10–15 min) (see Figure 4D). Other neurotoxins active at different SNARE proteins (e.g., BoNT-C for syntaxin) also cleave SNAP25 (e.g., Schiavo et al., 2000), precluding further study of these aspects. Therefore, these results suggest that SNAP25 could likely regulate KAR trafficking in a SNARE-independent manner. The data further indicate that SNAP25 in the postsynaptic compartments could be specifically involved in the protein interactions regulating internalization of GluK5-containing synaptic KARs.

SNAP25 Overexpression Increases Internalization of GluK5/GluK1$_{2a}$ KARs

To investigate SNAP25 possible effects on KAR internalization by an independent approach, we followed the endocytosis of the transfected myc-GluK5/GluK1$_{2a}$ receptors in the HEK293 cells (Figure S5) and hippocampal neurons (Figure 5) transfected with N-terminal EGFP-tagged SNAP25 constructs. Forty-eight hours following the transfection, live cells were labeled for surface-expressed myc-tagged GluK5 subunit. KARs were activated with 10 μM kainic acid (KA) for 2 min at 37°C. Cells were washed and left at 37°C for 10 min to allow the endocytosis of the myc-antibody labeled receptors. Cells were subsequently washed, fixed, and then incubated with Alexa 555-conjugated goat anti-mouse IgG to visualize the receptors remaining on the cell surface. After washing and permeabilization steps, the incubation was continued with Alexa 647-conjugated secondary antibody to label the internalized

GluK5 receptors and the receptors remaining on the cell surface. Internalization was measured as a ratio between the fluorescence intensity of Alexa 647 secondary antibody subtracted from the Alexa 555 antibody signal in the regions of overlap on the cell surface (to identify only the internalized receptor pool), and the intensity of the total Alexa 555 secondary antibody. The analysis of the collected data indicated that HEK293 cells coexpressing EGFP-SNAP25 construct displayed significantly larger levels of internalized GluK5 receptors (ratio of 0.59 ± 0.04; n = 205) than the cells coexpressing EGFP empty vector (0.33 ± 0.02; n = 145; p < 0.0001) (see Figure S6). Similarly, endocytosis of myc-GluK5-containing KARs in hippocampal neurons was more prominent in the cells overexpressing SNAP25 (intracellular to surface ratio of 1.13 ± 0.1; n = 102 ROIs from 20 neurons in three independent experiments) than in those cells in which exogenous SNAP25 was not present (0.56 ± 0.06; n = 102 ROIs from 28 neurons) (Figure 5B). Cleavage of SNAP25 by BoNT-A seems to impair SNAP25 function to stimulate KARs internalization. Therefore, we further assessed this result by overexpressing EGFP-SNAP25Δ9, a mutant missing the last nine amino acids that represents the truncated version of SNAP25 corresponding to the BoNT-A cleavage product (Schiavo et al., 1993). In neurons overexpressing this SNAP25 mutant, degree of internalization of KARs was found similar to controls (0.65 ± 0.04; n = 55 ROIS from 11 neurons) (Figures 5A and 5B). Furthermore, association of this mutant with GluK5 in BIFC experiments was significantly reduced, although not eliminated (BIFC index was attenuated approximately by 25%: from 46 ± 2.0, n = 90, to 34 ± 1.5, n = 102, p < 0.001; data not shown). These results suggest that overexpression of EGFP-SNAP25 is able to engage in additional functional protein complexes and so increase the rate of endocytosis of GluK5 receptors and that for this function SNAP25 requires the last nine amino acids of its C-terminal domain.
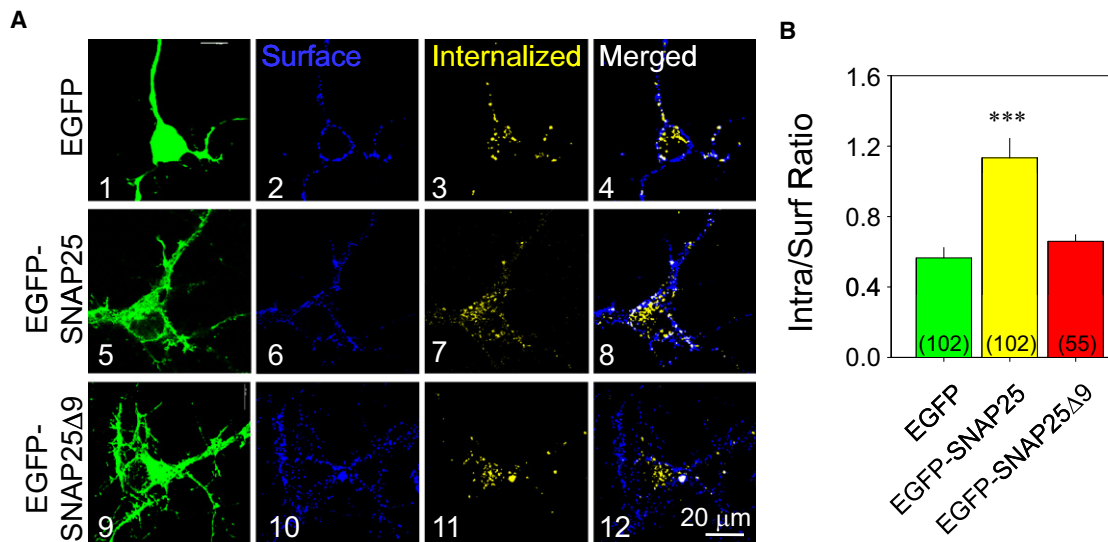
Figure 5. Expression of SNAP25 Facilitates Internalization of GluK5-Containing Receptors in Cultured Hippocampal Neurons
(A) Overexpression of SNAP25WT but not SNAP25 C-terminal deletion mutant (SNAP25Δ9) facilitates internalization of GluK5-containing receptors in cultured hippocampal neurons. Neurons were transfected at DIV8–10, and the internalization of Myc-tagged GluK5/GluK1$_{2a}$ receptors analyzed 48 hr later. Endocytosis of myc-tagged GluK5 subunit was visualized and quantified by the immunofluorescence internalization assay after 2 min exposure to 10 μM kainate followed by 10 min endocytosis. Prelabeled myc-GluK5 receptor subunits remaining on the surface are in blue and the internalized receptors in yellow.
(B) Quantification of GluK5 internalization measured as the ratio of internalized (yellow)/surface (blue) fluorescence. The data represent the results collected from three independent experiments. Bars are means ± SEM; ***p < 0.0001, unpaired Student's t test.

SNAP25-GluK5 Interactions Can Be Disrupted by Peptides

The last C-terminal nine amino acids of SNAP25 are not involved in SNARE complex assembly but rather serve for coupling SNARE function to calcium stimuli via synaptotagmin (O'Connor and Lee, 2002). The action of BoNT-A and the absence of effect of EGFP-SNAP25Δ9 on myc-GluK5 endocytosis in neurons indicate that SNAP25 C-terminal nine amino acids are important for SNAP25 interactions with GluK5 receptor or other receptor interacting proteins. In electrophysiological assays, the effects of a peptide containing the last nine amino acids of SNAP25 (Figure 6A), but not of this peptide scrambled, was similar to the action of SNAP25 antibodies in that it produced a run-up of EPSC$_{KAR}$ recorded from CA3 pyramidal neurons (Figure 6B). We further used a 6 aa peptide mimicking N-terminal sequence of SNAP25, that interferes with the interaction of SNAP25 with partner proteins (DD04107) (Blanes-Mira et al., 2004). DD04107 (50 μM) also produced an enhancement of 175.3% ± 17.6% at 15 min after break in (n = 10; p < 0.01) (Figure 6C). The action of C-terminal peptide was weaker, since at 100 μM C9 did increase KAR-mediated EPSC but without reaching statistical significance (136.7% ± 7.4%; n = 8) as compared to the scrambled peptide (117% ± 9.8%, n = 7; p = 0.17), both measured at 5–8 min after break in. However, at 200 μM the C9 peptide did efficiently enhanced KAR-mediated EPSC (188.9% ± 29%; n = 12; p < 0.05) (Figures 6B and 6C). The action of these peptides was specific for KARs, since AMPAR-mediated EPSC were largely unaffected in similar experiments (Figure S6). To demonstrate that these peptides decreased the SNAP25 to GluK5 interaction, we performed pull downs from brain homogenate using GST-GluK5$_{825-979}$ preincubated with

the SNAP25 peptides in the presence of ATP and Mg^{2+} (Figure 6D). SNAP25 binding to GST-GluK5 was significantly reduced in the presence of N- and C-terminal peptides (to 62.3% ± 5.9% and 59.0% ± 4%, respectively; p < 0.01) compared to the binding in the absence of peptides, whereas a scrambled version of the C9 peptide did not significantly reduce the binding of SNAP25 (to 84.2% ± 9.4%; p = 0.22). Importantly, N- and C-terminal peptides did not reduce PICK1 binding to GST-GluK5$_{825-979}$. (p ≥ 0.15) (Figures 6D and 6E).

Taken together, these data imply that both N- and C-terminal SNAP25 peptides may be important for SNAP25 interactions with GluK5 and that PICK1 binding to GluK5 is independent of SNAP25.

Disruption of SNAP25-GluK5 Interaction Prevents Long-Term Depression of EPSC$_{KAR}$

We then wondered whether this interaction would play any effect on activity dependent regulation of synaptic transmission. To this end, we looked for an experimental situation in which the efficacy of CA3 synaptic transmission would change as a consequence of a postsynaptic modification. As it is well known, mossy fiber to CA3 synapses show plastic changes mainly based on presynaptic alterations (e.g., Nicoll and Schmitz, 2005), which result in changes in the release probability of glutamate. However, it has been recently shown that some components (i.e., NMDA receptors) of these synapses could also undergo forms of plasticity that is expressed postsynaptically (Kwon and Castillo, 2008; Rebola et al., 2008). Therefore, we tested several protocols of synaptic stimulation and found that activation of mossy fibers for a period of 15–20 min while holding the membrane of CA3 pyramidal cells at +30 mV, resulted in
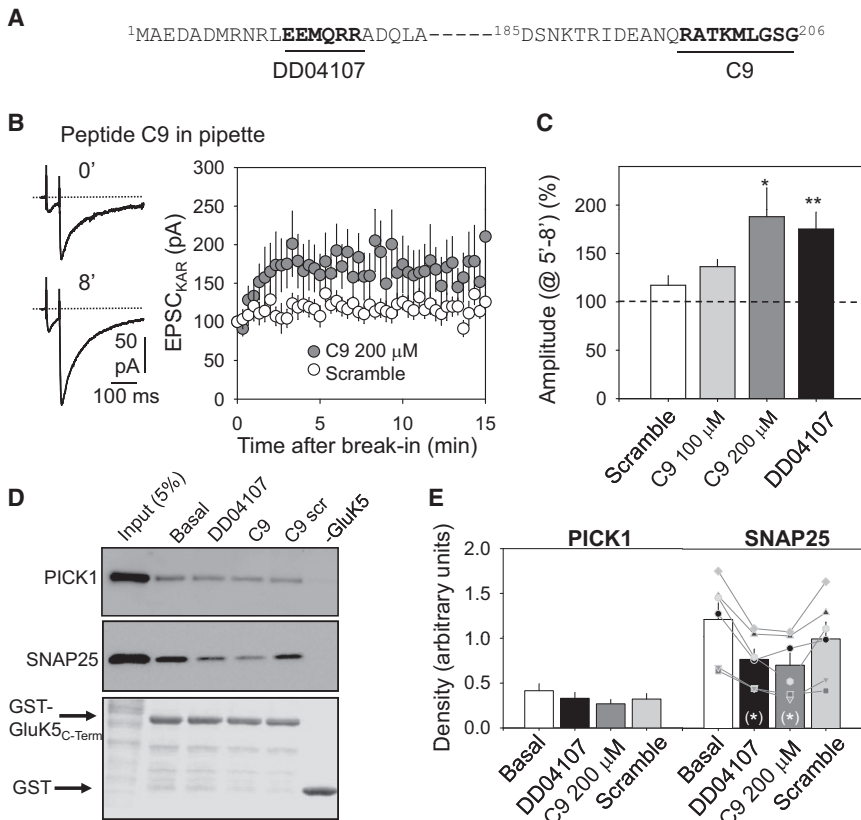
A

^{1}MAEDADMRNRL**EEMQRR**ADQLA-----^{185}DSNKTRIDEANQ**RATKMLGSG**^{206}

DD04107   C9

Figure 6. Blockade of SNAP25 Interaction with GluK5 by Inhibitory Peptides Increases KAR Synaptic Responses

(A) The SNAP25 N- and C-terminal peptides used to interfere with the interaction of SNAP25 and GluK5 receptors are indicated. A scrambled peptide (TGKRLSAGM) was used as a control.

(B) Dialysis of SNAP25 peptides from the whole-cell recording pipette caused an increase in the size of EPSCs mediated by KARs. Records (left) are average responses obtained at the beginning of the recording (0 min) and 8 min after dialysing C9 peptide (200 μM).

(C) Summary of data obtained in 7–12 neurons. DD04107 was introduced at 50 μM concentration. *p < 0.05, **p < 0.01, Student's t test.

(D) Inhibition of SNAP25 binding to GST-GluK5 in the presence of N- and C-terminal peptides. GST-GluK5$_{825-979}$ was preincubated with N-terminal (DD04107), C-terminal (C9), or the control C9 scrambled peptide under phosphorylation conditions (1 mM ATP/2 mM MgCl$_2$) and bound proteins analyzed by SDS-PAGE and immunoblotting. Nitrocellulose membranes were stained with Mem-Code protein stain to visualize GST-GluK5$_{825-979}$ and GST proteins (bottom panel).

(E) All values were normalized to the amount of GST-GluK5$_{825-979}$ retained on the beads and the percentage of binding expressed as the percentage of the corresponding "basal" value obtained in the absence of peptides. Both peptides decreased the binding of SNAP25 to the C-term of GluK5 (*p < 0.05, Student's t test; single data points are superimposed to the mean values illustrated by bars) but not that of PICK1 (p ≥ 0.2).

All values represent the means ± SEM.

a long-lasting depression of KAR-mediated EPSCs (Figure 7A) (37.4% ± 3.8% of depression, n = 17 cells from 17 slices; p < 0.01). Similar results were obtained with no postsynaptic depolarization but faster stimulation rate (300 stimuli delivered at 1 Hz) (36.0% ± 7.5% of depression; n = 12, p < 0.05) (Figure 7B). Notably, this pattern of synaptic activation was insufficient to induce LTD of AMPA receptor component (after induction protocol, the response was 93.2% ± 12.3% of the previous, n = 8) (Figure 7D). Similarly, depolarization without synaptic stimulation did not produce any significant change in the amplitude of EPSC$_{KAR}$ (data not shown). Activation of NMDA receptors was not a requisite, since this LTD could also be induced in the presence of APV (50 μM). We assessed this kind of LTD of EPSC$_{KAR}$ as of postsynaptic origin, since paired-pulse ratio, a common parameter used to evaluate the involvement of presynaptic phenomena, showed negligible changes in either case (3.53 ± 0.34 versus 3.32 ± 0.37; 3.21 ± 0.30 versus 3.61 ± 0.47 before and after LTD, respectively, for one and the other protocol; see Figure 7C for pooled data: 3.38 ± 0.30 versus 3.34 ± 0.29, n = 20). Interestingly, this postsynaptic EPSC$_{KAR}$ LTD was never seen in slices from GluK5-deficient mice (Figure 7E), indicating the requirement of this subunit for this specific form of plasticity. To determine whether EPSC$_{KAR}$ LTD required the interaction of GluK5 with SNAP25 at a postsynaptic level, we introduced in the pipette the peptide DD04120, the

N-terminal SNAP25 peptide that efficiently antagonized SNAP25 to GluK5 interaction in biochemical assays. Induction of EPSC$_{KAR}$ LTD was largely prevented by this peptide (16.6% ± 6.2% of depression; n = 8 slices, p < 0.05 compared to intermingled controls: 38.1% ± 4.9%, n = 9) (Figure 7F).

Taken together, these results indicate that KAR-mediated synaptic transmission at mossy fiber to CA3 neurons undergo activity-dependent endocytosis, a phenomenon that results in long-term depression of synaptic strength, requiring the interaction of GluK5 subunits with SNAP25.

PKC-Mediated Phosphorylation Regulates SNAP25 and PICK1 Interactions with GluK5

Since an experimental situation favoring phosphorylation activity (e.g., adding ATP + Mg^{2+}) drastically incremented interaction of SNAP25 to GluK5 (see Figure 1D) and trafficking of both AMPA and KARs has been previously shown to be regulated by the PKC activity (Martin and Henley, 2004; Perez et al., 2001), we wondered whether SNAP25 to GluK5 interaction is actually regulated by PKC-mediated phosphorylation. Using the group phosphorylation scoring method (Xue et al., 2005), we identified eight putative PKC consensus phosphorylation sites within GluK5 C terminus. Interestingly, SNAP25 and PICK1 are also possible targets and the latter also interacts with PKC (Staudinger et al., 1997).
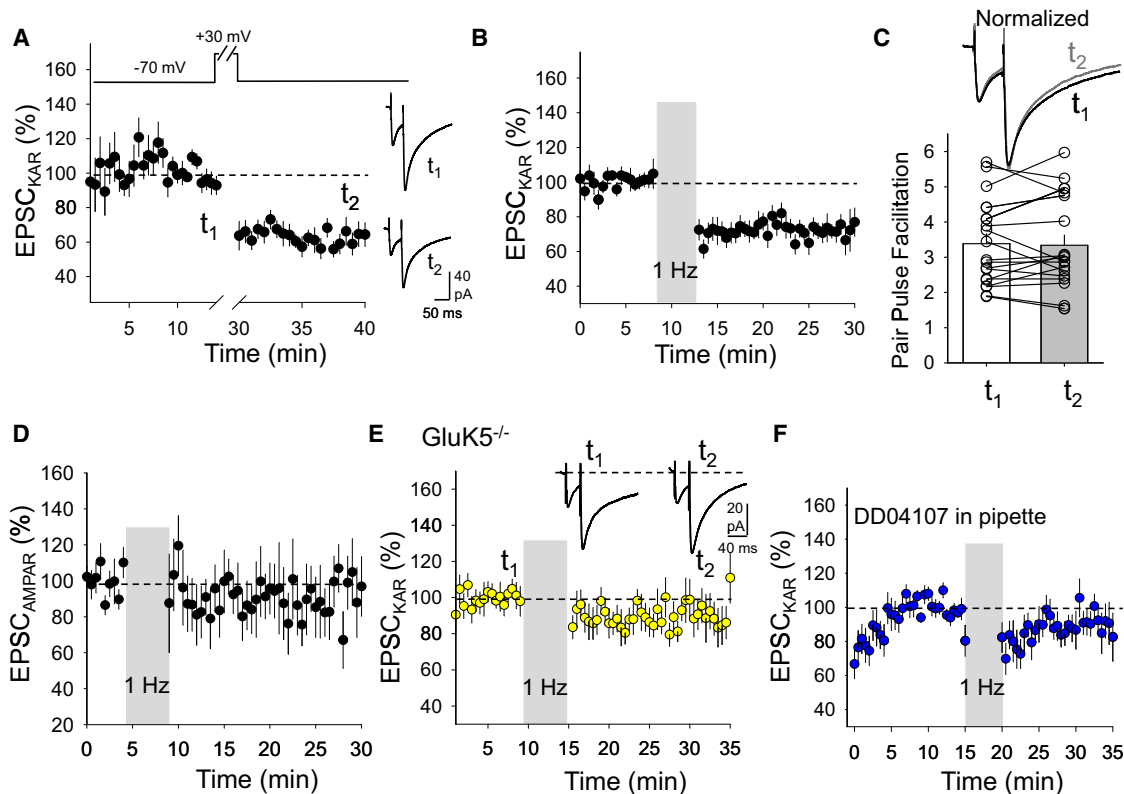
Figure 7. GluK5-Dependent Postsynaptic Long-Term Depression of KAR-Mediated EPSC in Mossy Fiber to CA3 Synapses
Both, 15 min depolarization (+30 mV) during continuous 0.1 Hz stimulation (A) or 1 Hz stimulation during 5 min (300 pulses) at hyperpolarized potentials (B) induced LTD of KAR-mediated EPSCs. (C) Paired-pulse ratio remained constant throughout the experiment, indicating the lack of any change in transmitter release. (D) These protocols of $EPSC_{KAR}$ LTD induction were ineffective for inducing LTD of synaptic component mediated by AMPARs. (E) $EPSC_{KAR}$ LTD was absent in GluK5-deficient mice. (F) Introduction of the N-terminal SNAP25 peptide, DD04107, in the recording pipette prevented LTD of KAR-mediated EPSC. Note the earlier run-up of $EPSC_{KAR}$ due to the disruption of SNAP25:GluK5 interaction. All values represent the means ± SEM.

Using a GST-tagged construct encoding the C terminus of GluK5 (GST-GluK5$_{825-979}$), we carried out pull-down assays from mouse hippocampal homogenate under conditions either promoting or inhibiting protein phosphorylation (Figures 8A and 8B). The interaction of GST-GluK5$_{825-979}$ with SNAP25 was drastically enhanced when ATP and Mg^{2+} were included in the solution, a situation favoring protein phosphorylation. A robust PICK1 binding to the GluK5 C terminus was also observed under these circumstances, whereas GRIP binding was either weak or absent. VAMP-2/synaptobrevin was not detected in the complexes pulled down by GST-GluK5$_{825-979}$. However, a clear signal for syntaxin-1 was apparent although exclusively under phosphorylating conditions, whenever interaction of GluK5 with SNAP25 was largely stimulated. Therefore, the well-known interaction of syntaxin with SNAP25, rather than a direct pull down by GluK5, may be responsible for this result. The fact that a GluK5 antibody did not coimmunoprecipitate syntaxin (see Figure 1A) further supports this idea.

Interestingly, the ATP-Mg^{2+}-dependent stimulation of protein interaction with GluK5 was greatly attenuated when the PKC inhibitor calphostin C was included during the pull-down assay (Figures 8A and 8B). These results indicate that SNAP25, GluK5, and PICK1 may form a complex under adequate phos-

phorylation conditions. To verify these results by a different approach in vivo, we transfected the undifferentiated SHSY5-Y cells with myc-GluK5 and GluK1$_{2a}$ in order to carry out coimmunoprecipitation with anti-myc antibody under PKC activation (Figure 8C). Undifferentiated SHSY5-Y cells express endogenously SNAP25, PICK1, and GRIP but do not express kainate receptors (Figure S7). Forty-eight hours after transfection, cells were incubated with 100 nM phorbol 12-myristate 13-acetate (TPA) while they were stimulated with 10 μM KA for 2 min. SNAP25 binding was increased by 38% ± 4% (n = 3 assays) in TPA-stimulated cells compared to control conditions (p < 0.05; unpaired t test) (Figures 8C and 8D), and no SNAP25 was detected in the myc-antibody immunoprecipitates from the cells transfected with the empty myc-vector. PICK1 binding to myc-GluK5 was similarly increased in the TPA-stimulated cells by 44% ± 2% (p < 0.05; unpaired t test, n = 3). Taken together, these results indicate that both SNAP25 and PICK1 engage in the GluK5-associated protein complexes induced by phosphorylation-dependent events and that this association is regulated, at least in part, by PKC activity. Indeed, PKC regulation of GluK5/SNAP25/PICK1 interactions has functional consequences, since the inhibition of PKC by introducing calphostin C (1 μM) or bisindolylmaleimide (0.1 μM) through the patch pipette induced a run
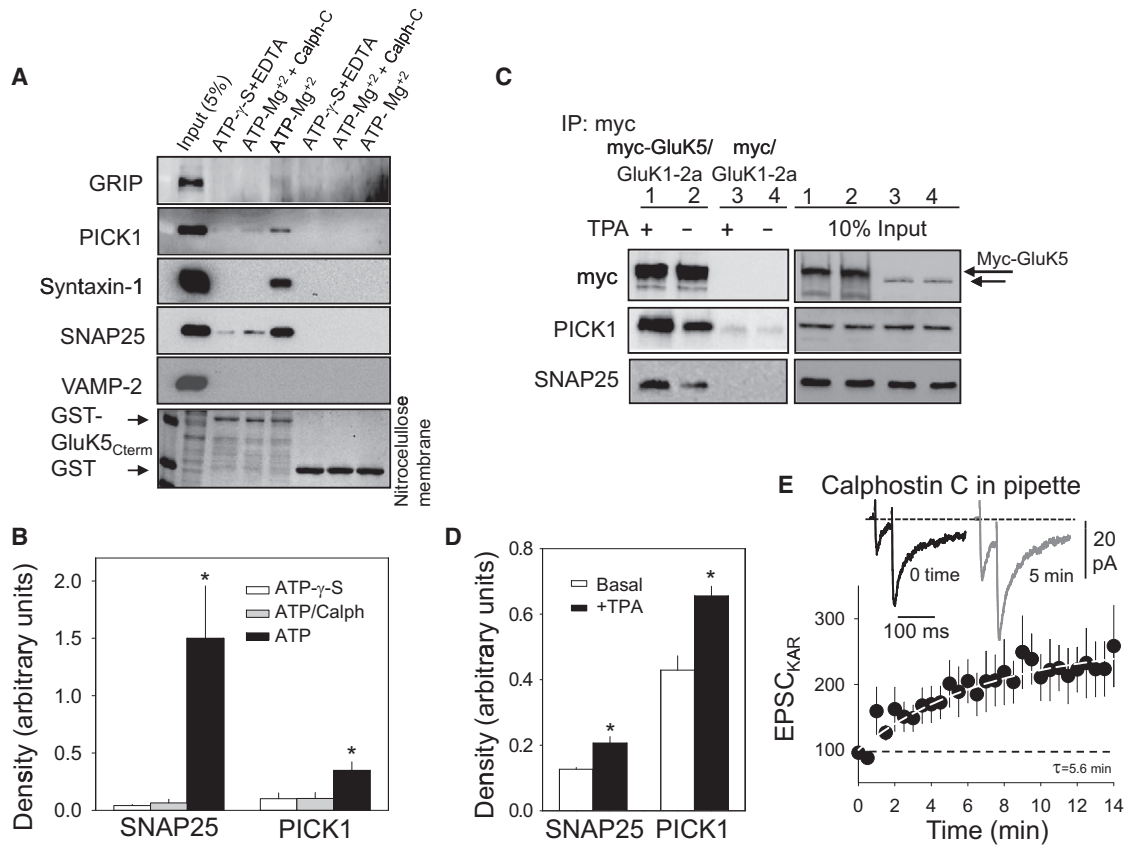
Figure 8. PICK1 and SNAP25 Binding to GluK5 Is Phosphorylation Dependent and Involves Protein Kinase C
(A) SNAP25 and PICK1 binding to the C terminus of GluK5 is promoted by ATP hydrolysis. GST-tagged GluK5 C-terminal domain or GST tag alone were bound to glutathione sepharose beads and incubated with mouse brain homogenate under indicated conditions. Beads were analyzed by western blot using the indicated antibodies.
(B) Summary data from three independent experiments, quantitated by scanning densitometry.
(C) Stimulation of PKC activity enhances PICK1 and SNAP25 binding to GluK5 heteromeric receptor in SHSY5-Y transfected cells. Receptor internalization was induced with 10 μM KA with or without a prior stimulation with TPA (see Experimental Procedures). Coprecipitation of SNAP25 and PICK1 with GluK5 receptor subunits was significantly enhanced in TPA-treated cells (lane 1) compared to control conditions (lane 2).
(D) Summary of data of SNAP25 and PICK1 increased binding to myc-GluK5 in the TPA-stimulated cells (by 38% ± 4% and 44% ± 2%, respectively, compared to controls; *p < 0.01 unpaired Student's t test, n = 3). The IP band densities were normalized to their corresponding lysate (Input) band density.
(E) Inhibition of PKC activity by introducing calphostin C (1 μM) in the patch pipette during recordings of the mossy fiber evoked EPSC$_{KA}$ produced a run up of the synaptic response, presenting an exponential time course with an ≈5 min of time constant.
All values represent the means ± SEM.

up of the EPSC$_{KA}$ responses in CA3 pyramidal neurons (reaching 234.3% ± 45%; n = 9; for calphostin C and 236.1% ± 78.5% for bisindolylmaleimide, n = 3, of initial responses in 14–15 min) (Figure 8E). Interestingly, inhibition of PKC by intrapipette calphostin C or bisindolylmaleimide also attenuated development of EPSC$_{KAR}$ LTD in CA3 neurons (16.7% ± 6.1%, n = 9, and 21.8 ± 5.4, n = 3, respectively, compared to 36.4% ± 6.1% of LTD in intermingled controls, n = 10; p < 0.05; Figure 9A), indicating that PKC activity is also required for this form of plasticity to occur.

EPSC$_{KAR}$ LTD in CA3 Neurons Requires the Synaptic Activation of Metabotropic Glutamate Receptors
It is well known that a major form of LTD requires activation of either NMDARs or mGluRs (e.g., Mulkey and Malenka, 1992;

Bashir et al., 1993). In the present experiments, LTD of EPSC$_{KAR}$ was effectively induced in the presence of NMDAR blockers. Therefore, we decided to test whether activation of mGluRs was required, since it would result in both activation of PKC and Ca^{2+} release from intracellular stores, both actions favoring the formation of GluK5/SNAP25/PICK1 complex. To study the involvement of mGluRs, we applied protocols inducing EPSC$_{KAR}$ LTD in the presence of the selective MGluR1 antagonist, MPEP (4 μM). As shown in Figure 9B, we were unable to induce LTD of the KAR-mediated component in slices bathed with this antagonist (average response was 97.4% ± 9.7%, n = 8) as compared to intermingled control slices (128.0% ± 7.0%, n = 6; p < 0.05). We also chelated Ca^{2+} in the postsynaptic neuron by introducing a high concentration of BAPTA in the recording pipette, which has been shown to prevent the
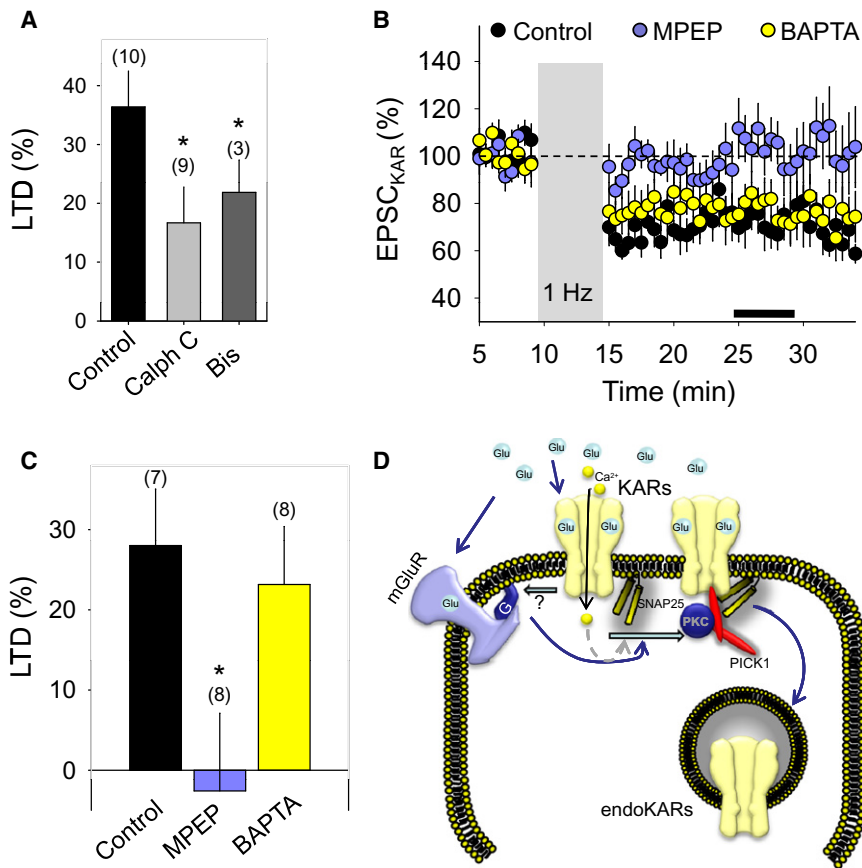
Figure 9. Signaling Dependence of EPSC$_{KAR}$ LTD

(A) Postsynaptic inhibition of PKC prevented LTD of EPSC$_{KAR}$ as compared to control intermingled slices (*p < 0.05, Student's t test). In these experiments, calphostin C (1μM) or bisindolylmaleimide (0.1 μM) were included in the recording pipette. After reaching a steady state in EPSC$_{KAR}$, LTD inducing protocol was applied.

(B) Blockade of mGluR5 with bath applied MPEP (1 μM) totally prevented LTD of EPSC$_{KAR}$ in mossy fiber to CA3 synapses. However, chelating intracellular Ca^{2+} by including in the pipette 20 mM BAPTA did not.

(C) Summary data calculated at the time indicated in (B) by a horizontal bar. Numbers in parenthesis indicate slices analyzed. *p < 0.05, Student's t test.

(D) A cartoon illustrating the putative role of mGluRs, SNAP25, PICK1 and PKC in long-term synaptic kainate receptor internalization.

All values represent the means ± SEM.

induction of LTD induced by mGluR stimulation in other synapses (Cho et al., 2000). Surprisingly, we found that BAPTA (up to 20 mM) did not prevent the induction of EPSC$_{KAR}$ LTD using our induction protocols (123.1% ± 7.2%, n = 8, p = 0.64) (Figures 9B and 9C).

These results indicate that while activation of PKC required for endocytosis of synaptic KARs may be driven by mGluR activity, the release of Ca^{2+} subsequent to mGluR activation seems to be not necessary for this phenomenon to occur, in clear contrast to what has been found for LTD of AMPAR component in other systems (e.g., Jo et al., 2008).

DISCUSSION

We have found a role for SNAP25 in the regulation of dynamic synaptic turnover of kainate-type glutamate receptors. Blocking SNAP25 function by SNAP25-specific antibodies, BoNT-A toxin cleavage and small N- or C-terminal peptides led to an increase of KAR-mediated EPSCs recorded in the hippocampal CA3 pyramidal neurons, an effect that was absent in the *GluK5*$^{-/-}$ mice. Biochemical experiments revealed the interaction of SNAP25 with GluK5 subunits, which was further confirmed by bimolecular fluorescence complementation, a technique that allows detection of protein-protein in vivo interactions (Kerppola, 2006; Saka et al., 2007). Our data also indicate that SNAP25 and GluK5 likely form a complex with the well-known trafficking proteins PICK1 and GRIP at a postsynaptic level. This complex

seems to be regulated by PKC phosphorylation, such that stimulation of PKC by synaptic mGluRs triggers a form of long-term depression of KAR-mediated synaptic responses, specifically involving SNAP25 and GluK5 interactions.

Indeed, SNAP25 overexpression in neurons and epithelial cells increased the intracellular accumulation of GluK5 heteromeric receptors, an effect that was not detected with a C-terminal SNAP25 deletion mutant. The most reasonable explanation for these results is the involvement of SNAP25 in the internalization of synaptic KARs, a phenomenon that requires KARs incorporating GluK5 subunits. Our data also imply that internalization of GluK5 receptors involves PKC-regulated interactions with the PKC-interacting protein PICK1. Thus, the regulated interaction of GluK5 with known (PICK1 and GRIP) and new (SNAP25) scaffolding proteins results in the activity-dependent regulation of KARs in the postsynaptic membrane. The failure of clostridial toxins, such as BoNT-B and tetanus Tx, affecting other SNARE proteins (e.g., VAMP-2/synaptobrevin) to prevent SNAP25-mediated internalization of KARs could indicate, in principle, that these actions may be independent of the SNAP25 role as a SNARE protein. Unfortunately, other toxins, such as BoNT-C that cleaves syntaxin, also affect SNAP25 (Niehmann et al., 1994; Rossetto et al., 2001), precluding further assessment of any specific details of the mode by which SNAP25 may regulates KAR activity through a SNARE-dependent or -independent mode. Nevertheless, our data identify a selective mechanism for regulating synaptic transmission at mossy fiber to CA3 synapses, in which SNAP25 allows the process of internalization of GluK5-containing receptors, a phenomenon that could be triggered in an activity-dependent manner.

Interaction of SNAP25 with GluK5 was undeniably weak and coimmunoprecipitation of both proteins rendered faint bands. This interaction was very much improved when brain homogenates were probed with the GluK5 C-terminal domain fused to

GST in pull-down assays, particularly when conditions were set to allow protein kinase activity (e.g., adding ATP-Mg^{2+}). Perhaps the availability of SNAP25 uncomplexed with the SNARE complex (i.e., free SNAP25) is very limited. This could be why the coimmunoprecipition renders weak signals. This could also partially account for why the interaction signal increases significantly in GST-pull-down analysis. The relatively new technique of bimolecular fluorescence complementation (BiFC) (Kerppola, 2006), developed to demonstrate protein-protein interaction in vivo, however, demonstrated readily formation of SNAP25-GluK5 complexes. BiFC takes advantage of the fact that when the two nonfluorescent halves of a fluorescent protein (e.g., YFP) are brought into close apposition they interact, leading to the irreversible formation of a fluorescent protein (i.e., Kerppola, 2008). As previously shown by using optimized BiFC assay with the YFP variant Venus (Saka et al., 2008), this technique could easily reveal the formation of protein complexes even if only a fraction of each protein interacts (Saka et al., 2007). Indeed, BiFC revealed a substantial degree of interaction between SNAP25 and GluK5, a phenomenon absolutely requiring the C-terminal domain of GluK5 (see Figure 1E). Weak interactions among two proteins may reflect indirect interaction. However, it is also possible that it is indicative of a rather dynamic functional process. Considering the striking effect that intracellular manipulation of SNAP25-GluK5 interaction has on KARs synaptic function, we are tempted to speculate that some protein-protein interactions could be intrinsically weak or transient should they serve a physiological regulatory mechanism. From a functional point of view, such a weak interaction may still be very significant.

PICK1 was first identified as a protein that interacts with PKCα (Staudinger et al., 1997) and regulates surface expression and clustering of AMPA receptors at synapses via PKC-dependent phosphorylation (Matsuda et al., 1999; Xia et al., 1999). PICK1 activity is additionally regulated by PKC, which induces PICK1 translocation to dendritic spines (Perez et al., 2001). It appears that PICK1 does not determine the direction of the receptor movement, but rather serves as an adaptor protein that recruits additional molecules associated with either exo- or endocytic pathway, depending on a specific stimulus or a cell type, as observed with AMPA receptors (Perez et al., 2001; Terashima et al., 2004; Gardner et al., 2005). Since SNARE proteins do not seem to determine membrane fusion specificity either (Yang et al., 1999; Pelham, 2001; Brandhorst et al., 2006), it is likely that like PICK1, SNAP25 facilitates endo- or exocytosis depending on a complex interplay of additional factors controlling the synaptic activity of a given receptor. Indeed, SNAP25 has been implicated in the PKC-dependent exocytosis of NMDA receptors (Kwon and Castillo, 2008; Lan et al., 2001), and also in endosomal fusion (Söllner et al., 1993; Pooley et al., 2006). Our finding that PICK1 can be immunoprecipitated in a complex with SNAP25 and GluK5 under conditions favoring PKC phosphorylation support the idea that PICK1 targeting to the synaptic membrane and its association with KARs and SNAP25 induces PKC-dependent endocytosis of surface receptors (see cartoon in Figure 9D).

Previous studies have shown that blocking endogenous PKC activity reduces EPSC$_{KAR}$ at mossy fiber synapses (Hirbec et al. 2003) and perirhinal cortex (Park et al. 2006). In addition, KAR signaling seems to be enhanced by activation of group I mGlu receptors in a PKC-dependent manner in perirhinal cortical neurons (Park et al., 2006). In the present study, however, we observed somehow opposite results in that PKC inhibition enhanced KAR-mediated synaptic transmission at mossy fibers, and PKC-stimulated interaction of GluK5 containing receptors with trafficking proteins, such as PICK1 and SNAP25, as evidenced by biochemical data, produced the long-term run down of EPSC$_{KAR}$ in an activity-dependent manner. It is difficult to figure out the reason for these discrepancies. In some cases, different synapses might behave in a completely opposite manner even using the same elements. In addition, interfering with different receptor subunits may also be a cause of dissimilarity. For instance, in Hirbec et al. (2003), reagents were developed to interfere with GluK1/GluK2-interacting proteins in CA3 neurons, and in perirhinal neurons KARs seems to include GluK1 subunits. In contrast, our experiments exclusively involved GluK5 interactions. Bath application of PKC inhibitors rather than their localized intracellular infusion may also be a reason for this discrepancy. Finally, induction of EPSC$_{KAR}$ LTD in perirhinal cortex requires a rise in postsynaptic Ca^{2+} from a release from stores (Park et al., 2006). The EPSC$_{KAR}$ LTD we describe differs in that, although dependent on mGluR signaling, it did not require a significant Ca^{2+} rise (Figure 9B). Thus, although a clear answer does not emerge at this point, our findings are entirely consistent with the existence of a particular form of long-term plasticity, tuning neurotransmission in a site- and receptor-specific manner (e.g., Kidd and Isaac, 1999; Rivera et al., 2007).

GluK5 subunits combine with other KAR subunits to make channels displaying functional properties different from KAR (e.g., GluK2) homomeric receptors (see Lerma, 2003, for a review). Interestingly, GluK5 is the only KAR subunit containing the endocytic dileucine motif within its C terminus (Ren et al., 2003). Dileucine motifs are recognized by clathrin adaptor proteins, which initiate receptor endocytosis by recruiting additional endocytic machinery (Sorkin, 2004). Therefore, it is conceivable that GluK5 could regulate the dynamic turnover of KARs at the cell surface, similar to the clathrin-dependent endocytosis reported for AMPA receptors (Barry and Ziff, 2002). Our data implicating PICK1 and SNAP25 in this process support the studies in which both PICK1 (Perez et al., 2001; Song and Huganir, 2002) and SNAP25 (Pooley et al., 2006; Sun et al., 2003) were implicated in the recycling of surface receptors. Therefore, our finding that the expression of exogenous SNAP25 increases KAR internalization supports the interpretation that blocking SNAP25 may interfere with the endocytosis of KARs.

Because KARs likely cycle rapidly between intracellular and plasma membranes, the amount of internalized receptor is strongly affected by both the rate of recycling to the surface and by the rate of endocytosis. Since exogenous SNAP25 expression increases internalization of GluK5 subunits and although several models could exist, we favor the explanation that SNAP25 destabilizes surface-bound synaptic GluK5 receptors. However, the way in which SNAP25 promotes GluK5 receptors internalization is not clear at present, since synaptic removal of glutamate receptors is likely a two-step process, involving an initial lateral movement from synaptic sites followed by the endocytosis (Derkach et al., 2007). Therefore, various models of SNAP25 mediated effects on synaptic stability of receptors

may be envisioned. Since SNAP25 and GluK5 colocalize almost exclusively in the association with the plasma membrane (Figure S8), it is even possible that SNAP25 could play a role in the lateral movement or sorting of activated KARs into the lateral plasma membrane invaginations representing endocytic "hot spots" (Lu et al., 2007).

Although still hypothetical, a simple phosphorylation-dependent model of GluK5:SNAP25 interactions can be envisioned (see cartoon in Figure 9D). PICK1 may bring PKC to phosphorylate the GluK5 C terminus; this phosphorylation may induce a conformational change facilitating the association with SNAP25 and simultaneously decreasing GRIP binding affinity. Indeed, it is known that PICK1 and GRIP binding to the GluA2 subunit are mutually exclusive (Osten et al., 2000). Our model, however, contradicts the idea that PICK1 regulates the stability of KARs on the membrane (Hirbec et al., 2003). We favor the explanation that PICK1 together with SNAP25 regulates endocytosis of KARs because either blocking SNAP25 or preventing its binding to GluK5 subunit increases the KAR-mediated synaptic responses in brain slices, although alternative models are also possible. However, as in other models of activity-stimulated endocytosis of synaptic receptors, activation of mGluRs seems to be the key factor for association of SNAP25 with GluK5 subunits by stimulating PKC. On the other hand, Ca^{2+} release from intracellular stores subsequent to mGluR activation or Ca^{2+} influx through receptor channels do not appear to be required in this mechanism for LTD.

Although evident, we are still far from fully understanding the role of SNAP25 in glutamate receptor trafficking. Based on our results, it is conceivable that postsynaptic SNAP25 may be important for regulating a dynamic equilibrium among the glutamate receptors at a given synapse, thereby leading to adequate tuning of neurotransmission also at a postsynaptic level. Indeed, we have uncovered forms of synaptic activity that induce LTD of $EPSC_{KAR}$ at mossy fiber synapses. This specific change of strength in the KAR-mediated component of synaptic transmission could have clear physiological and behavioral consequences, since these synapses are strategically situated in the hippocampal trisynaptic circuit and are required for rapid acquisition of memories in novel environments and for some instances of memory recall (Nakashiba et al., 2008). Bidirectional modulation of different synaptic inputs (e.g., KARS versus AMPARs or NMDARs) in mossy fiber to CA3 field implies significant changes in integrative properties of CA3 neurons and therefore in the information transfer throughout the hippocampal circuit.

Delineation of the signaling pathways involved in the regulation of KAR function via their selective targeting and trafficking is crucial for understanding the tuning of the synaptic transmission and for the development of KAR-targeted therapies for diseases such as epilepsy. The identification of SNAP25 as a key element of this process should reveal important for this endeavor.

EXPERIMENTAL PROCEDURES

Immunoprecipitation, Immunoblotting, and Immunocytochemistry

Membrane extracts or subcellular fractions were prepared from the brain tissue of P21–P26 C57 mice, as previously described (Selak et al., 2006).

Immunoprecipitations were performed by incubating membrane preparations with 50% protein A/G-Sepharose slurry (Amersham Biosciences) at 4°C to eliminate nonspecific binding. Precleared supernatants were incubated with dimethyl pimelimidate dihydrochloride (DMP)-coupled rabbit anti-GluK5 (C8) (06-315, Upstate Biotechnology, Waltham, MA), rabbit anti-GluK5 (C20) (a kind gift from Dr. M. Darstein), and anti-SNAP25 antibodies (SMI 81, Sternberger Monoclonals) overnight at 4°C in the presence of BSA. Bound proteins were eluted from beads and then separated by electrophoresis on SDS-PAGE gels. Proteins were electrotransferred onto nitrocellulose membranes and probed with rabbit anti-GluK5 (C8), rabbit anti-Myc (ab9106, AbCam), rabbit anti-Hrs (Santa Cruz), goat anti-PICK1 (C20, Santa Cruz) and the monoclonal antibodies: anti-SNAP25, anti-GRIP (BD Biosciences), anti-VAMP2 (Chemicon), anti-syntaxin1 (Cl 78.3, Synaptic Systems), anti-GFP (B-2, Santa Cruz) and anti-FLAG M2 antibody (Sigma). Immunoreactive bands were visualized using horseradish peroxidase (HRP)-conjugated goat anti-mouse secondary antibody (Pierce), goat anti-rabbit and rabbit anti-goat secondary antibodies (Pierce). The band density was quantitated using a Bioimager apparatus and Quantity One software.

Immunocytochemistry was performed as previously described (Selak et al. 2006). Images were acquired with a glycerol immersion objective (63×) in a Leica Laser Confocal Microscope (Leica DMLFSA).

Cell Transfections and Endocytosis Studies

Cells were transfected using Lipofectamine2000. Following transfection (48 hr) cells were live-labeled with mouse anti-myc antibody 9E10 to allow endocytosis (3–10 min). Endocytosis was stopped and cells fixed. Surface-bound myc antibody was detected with a goat secondary antibody conjugated with Alexa 555, and then cells were washed and permeabilized with Triton X and labeled with a goat secondary antibody conjugated with Alexa 647. Immunofluorescence intensity of Alexa 555 (surface label) and Alexa 647 (surface + internalized receptors) were measured for both soma and dendrites. The percentage of the internalized receptors was expressed as a ratio of the normalized Alexa 647 and Alexa 555 fluorescence intensities. HEK293 cells were analyzed in the same way.

Molecular Biology

myc-GluK5 cDNA was obtained from Dr. John Marshall (Brown University, Providence, RI, USA), pRK5-GluK1₂ₐ and pRK5-GluK5 from Dr. Peter Seeburg (Max Planck Institute, Heidelberg, Germany), EGFP-tagged SNAP25wt and SNAP25Δ9 from Dr. Luis M. Gutierrez (Instituto de Neurociencias, Alicante, Spain), and GST-SNAP25 used for preadsorbing antibodies was from Dr. Tomas Sudhof (UT Southwestern Medical Center, USA). GST-tagged GluK5 C terminus (GST-GluK5$_{825-979}$) was generated by PCR using the following primers: forward GGT CAT GGA ATT CAT CTG GTC, reverse CAG TCA CTC GAG GCG CAC and pRK5-GluK5 as template. All mutants were subcloned into pGex6P1 vector (Pharmacia Biotech) using EcoRI and XhoI site. All PCR amplified sequences and constructs were verified by DNA sequencing.

BiFC Constructs

The N-terminal and C-terminal halves of a modified version of YFP variant Venus (T153M) were amplified by PCR from plasmids (pCS2+) containing VN154m9 (residues 1–154, T153M) and VC155 (residues 155–239), kindly provided by James C. Smith (University of Cambridge, UK) (see Saka et al. 2007), and cloned into pcDNA3 expression vector. The VC155 fragment was fused to the N terminus of SNAP25 with a ten amino acids linker (GSAGSTGSGSSG), while the VN154m9 fragment was fused to the C terminus of the myc-GluK5 and myc-GluK5ΔCt with linkers consisting of AGSTGSGSS-GAA and RYPSHWRPAA, respectively. The T153M mutation reduces significantly self-assembly of VN154 with its counterpart VC155 (Saka et al. 2007). A fusion protein of VC155 fused to the C terminus of GluK1₂ₐ was similarly generated (with AGSTGSGSSGAA as a linker). All the PCR-derived constructs were verified by sequencing and were transfected in HEK293 cells using FuGENE 6 transfection reagent (Roche Molecular Biochemicals).

GST Protein Binding Studies

GST-GluK5$_{825-979}$ recombinant protein, corresponding to the C-terminal domain of GluK5 fused to GST, was expressed in the protease-deficient

BL21 strain of *E. coli.* GST proteins were incubated with 200 μg hippocampal lysate in the buffer N (25 mM HEPES-KOH [pH 7.3], 150 mM KCl, 1% Triton X-100, 10% glycerol, 0.2% BSA, 1 mM DTT) in the presence of either 2 mM EDTA and 1 mM ATPγS, 2 mM MgCl$_2$ and 1 mM of hydrolysable ATP (Sigma), or 5 nM calphostin C and 1 mM ATP. Bound proteins were detected by SDS-PAGE and immunoblotting. For peptide inhibition studies, the following SNAP25 peptides were used: N-terminal, EEMQRR (a kind gift of Dr. Ferrer-Montiel, UMH, Spain); C-terminal, RATKMLGSG and scrambled, TGKRLSAGM, all synthesized without any modifications.

Electrophysiology

Transverse hippocampal slices were prepared from P16–P21 C57 mice, as described (e.g., Christensen et al., 2004). All experiments were performed at room temperature (22°C–25°C). The slices were continuously perfused with 124 mM NaCl, 3 mM KCl, 1.25 mM KH$_2$PO$_4$, 1 mM MgCl$_2$, 2 mM CaCl$_2$, 26mM NaHCO$_3$, and 10 mM glucose, pH 7.3 (300 mOsm). This solution was supplemented with combinations of picrotoxin (50 μM), APV (50 μM) and LY303070 (25 μM) to isolate synaptic responses mediated by KARs. Intracellular solution consisted of (in mM) 130 CsMeSO$_3$Cl, 4 NaCl, 10 HEPES, 0.2 EGTA, and 10 TEA, 5 QX-314, 2 ATP, and 0.5 GTP, (pH 7.3, 287 mOsm).

A more detailed account of experimental procedures and reagents can be found as Supplemental Data.

SUPPLEMENTAL DATA

Supplemental Data include detailed Experimental Procedures and eight figures and can be found with this article online at http://www.cell.com/neuron/supplemental/S0896-6273(09)00546-7.

REFERENCES

Barry, M.F., and Ziff, E.B. (2002). Receptor trafficking and the plasticity of excitatory synapses. Curr. Opin. Neurobiol. *12*, 279–286.

Bashir, Z.I., Bortolotto, Z.A., Davies, C.H., Berretta, N., Irving, A.J., Seal, A.J., Henley, J.M., Jane, D.E., Watkins, J.C., and Collingridge, G.L. (1993). Induction of LTP in the hippocampus needs synaptic activation of glutamate metabotropic receptors. Nature *363*, 347–350.

Baumert, M., Maycox, P.R., Navone, F., De, C.P., and Jahn, R. (1989). Synaptobrevin: an integral membrane protein of 18,000 daltons present in small synaptic vesicles of rat brain. EMBO J. *8*, 379–384.

Blanes-Mira, C., Merino, J.M., Valera, E., Fernández-Ballester, G., Gutiérrez, L.M., Viniegra, S., Pérez-Payá, E., and Ferrer-Montiel, A. (2004). Small peptides patterned after the N-terminus domain of SNAP25 inhibit SNARE complex assembly and regulated exocytosis. J. Neurochem. *88*, 124–135.

Brandhorst, D., Zwilling, D., Rizzoli, S.O., Lippert, U., Lang, T., and Jahn, R. (2006). Homotypic fusion of early endosomes: SNAREs do not determine fusion specificity. Proc. Natl. Acad. Sci. USA *103*, 2701–2706.

Cho, K., Kemp, N., Noel, J., Aggleton, J.P., Brown, M.W., and Bashir, Z.I. (2000). A new form of long-term depression in the perirhinal cortex. Nat. Neurosci. *3*, 150–156.

Christensen, J.K., Paternain, A.V., Selak, S., Ahring, P.K., and Lerma, J. (2004). A mosaic of functional kainate receptors in hippocampal interneurons. J. Neurosci. *24*, 8986–8993.

Collingridge, G.L., Olsen, R.W., Peters, J., and Spedding, M. (2009). A nomenclature for ligand-gated ion channels. Neuropharmacology *56*, 2–5.

Contractor, A., Sailer, A.W., Darstein, M., Maron, C., Xu, J., Swanson, G.T., and Heinemann, S.F. (2003). Loss of kainate receptor-mediated heterosynaptic facilitation of mossy-fiber synapses in KA2−/− mice. J. Neurosci. *23*, 422–429.

Coussen, F., Perrais, D., Jaskolski, F., Sachidhanandam, S., Normand, E., Bockaert, J., Marin, P., and Mulle, C. (2005). Co-assembly of two GluR6 kainate receptor splice variants within a functional protein complex. Neuron *47*, 555–566.

Cui, C., and Mayer, M.L. (1999). Heteromeric kainate receptors formed by the coassembly of GluK1, GluR6, and GluR7. J. Neurosci. *19*, 8281–8291.

Darstein, M., Petralia, R.S., Swanson, G.T., Wenthold, R.J., and Heinemann, S.F. (2003). Distribution of kainate receptor subunits at hippocampal mossy fiber synapses. J. Neurosci. *23*, 8013–8019.

Derkach, V.A., Oh, M.C., Guire, E.S., and Soderling, T.R. (2007). Regulatory mechanisms of AMPA receptors in synaptic plasticity. Nat. Rev. Neurosci. *8*, 101–113.

Garcia, E.P., Mehta, S., Blair, L.A., Wells, D.G., Shang, J., Fukushima, T., Fallon, J.R., Garner, C.C., and Marshall, J. (1998). SAP90 binds and clusters kainate receptors causing incomplete desensitization. Neuron *21*, 727–739.

Gardner, S.M., Takamiya, K., Xia, J., Suh, J.G., Johnson, R., Yu, S., and Huganir, R.L. (2005). Calcium-permeable AMPA receptor plasticity is mediated by subunit-specific interactions with PICK1 and NSF. Neuron *45*, 903–915.

Herb, A., Burnashev, N., Werner, P., Sakmann, B., Wisden, W., and Seeburg, P.H. (1992). The KA-2 subunit of excitatory amino acid receptors shows widespread expression in brain and forms ion channels with distantly related subunits. Neuron *8*, 775–785.

Hirbec, H., Francis, J.C., Lauri, S.E., Braithwaite, S.P., Coussen, F., Mulle, C., Dev, K.K., Coutinho, V., Meyer, G., Isaac, J.T., et al. (2003). Rapid and differential regulation of AMPA and kainate receptors at hippocampal mossy fibre synapses by PICK1 and GRIP. Neuron *37*, 625–638.

Huettner, J.E. (2003). Kainate receptors and synaptic transmission. Prog. Neurobiol. *70*, 387–407.

Jaskolski, F., Coussen, F., Nagarajan, N., Normand, E., Rosenmund, C., and Mulle, C. (2004). Subunit composition and alternative splicing regulate membrane delivery of kainate receptors. J. Neurosci. *24*, 2506–2515.

Jo, J., Heon, S., Kim, M.J., Son, G.H., Park, Y., Henley, J.M., Weiss, J.L., Sheng, M., Collingridge, G.L., and Cho, K. (2008). Metabotropic glutamate receptor-mediated LTD involves two interacting Ca(2+) sensors, NCS-1 and PICK1. Neuron *60*, 1095–1111.

Kerppola, T.K. (2006). Design and implementation of bimolecular fluorescence complementation (BiFC) assays for the visualization of protein interactions in living cells. Nat. Protocols *1*, 1278–1286.

Kerppola, T.K. (2008). Bimolecular fluorescence complementation: Visualization of molecular interactions in living cells. Methods Cell Biol. *85*, 431–470.

Kidd, F.L., and Isaac, J.T. (1999). Developmental and activity-dependent regulation of kainate receptors at thalamocortical synapses. Nature *400*, 569–573.

Kwon, H.B., and Castillo, P.E. (2008). Long-term potentiation selectively expressed by NMDA receptors at hippocampal mossy fiber synapses. Neuron *57*, 108–120.

Lan, J.Y., Skeberdis, V.A., Jover, T., Grooms, S.Y., Lin, Y., Araneda, R.C., Zheng, X., Bennett, M.V., and Zukin, R.S. (2001). Protein kinase C modulates NMDA receptor trafficking and gating. Nat. Neurosci. 4, 382–390.

Lerma, J. (2003). Roles and rules of kainate receptors in synaptic transmission. Nat. Rev. Neurosci. 4, 481–495.

Lu, J., Helton, T.D., Blanpied, T.A., Rácz, B., Newpher, T.M., Weinberg, R.J., and Ehlers, M.D. (2007). Postsynaptic positioning of endocytic zones and AMPA receptor cycling by physical coupling of dynamin-3 to Homer. Neuron 55, 874–889.

Martin, S., and Henley, J.M. (2004). Activity-dependent endocytic sorting of kainate receptors to recycling or degradation pathways. EMBO J. 23, 4749–4759.

Matsuda, S., Mikawa, S., and Hirai, H. (1999). Phosphorylation of serine-880 in GluR2 by protein kinase C prevents its C terminus from binding with glutamate receptor-interacting protein. J. Neurochem. 73, 1765–1768.

Mulle, C., Sailer, A., Pérez-Otaño, I., Dickinson-Anson, H., Castillo, P.E., Bureau, I., Maron, C., Gage, F.H., Mann, J.R., Bettler, B., and Heinemann, S.F. (1998). Altered synaptic physiology and reduced susceptibility to kainate-induced seizures in GluR6-deficient mice. Nature 392, 601–605.

Mulkey, R.M., and Malenka, R.C. (1992). Mechanisms underlying induction of homosynaptic long-term depression in area CA1 of the hippocampus. Neuron 9, 967–975.

Nakashiba, T., Young, J.Z., McHugh, T.J., Buhl, D.L., and Tonegawa, S. (2008). Transgenic inhibition of synaptic transmission reveals role of CA3 output in hippocampal learning. Science 319, 1260–1264.

Nicoll, R.A., and Schmitz, D. (2005). Synaptic plasticity at hippocampal mossy fibre synapses. Nat. Rev. Neurosci. 6, 863–876.

Niemann, H., Blasi, J., and Jahn, R. (1994). Clostridial neurotoxins: new tools for dissecting exocytosis. Trends Cell Biol. 4, 179–185.

O'Connor, V., and Lee, A.G. (2002). Synaptic vesicle fusion and synaptotagmin: 2B or not 2B? Nat. Neurosci. 5, 823–824.

Osten, P., Khatri, L., Perez, J.L., Köhr, G., Giese, G., Daly, C., Schulz, T.W., Wensky, A., Lee, L.M., and Ziff, E.B. (2000). Mutagenesis reveals a role for ABP/GRIP binding to GluR2 in synaptic surface accumulation of the AMPA receptor. Neuron 27, 313–325.

Park, Y., Jo, J., Isaac, J.T., and Cho, K. (2006). Long-term depression of kainate receptor-mediated synaptic transmission. Neuron 49, 95–106.

Paternain, A.V., Herrera, M.T., Nieto, M.A., and Lerma, J. (2000). GluK1 and GluR6 kainate receptor subunits coexist in hippocampal neurons and coassemble to form functional receptors. J. Neurosci. 20, 196–205.

Pelham, H.R. (2001). SNAREs and the specificity of membrane fusion. Trends Cell Biol. 11, 99–101.

Perez, J.L., Khatri, L., Chang, C., Srivastava, S., Osten, P., and Ziff, E.B. (2001). PICK1 targets activated protein kinase Calpha to AMPA receptor clusters in spines of hippocampal neurons and reduces surface levels of the AMPA-type glutamate receptor subunit 2. J. Neurosci. 21, 5417–5428.

Pooley, R.D., Reddy, S., Soukoulis, V., Roland, J.T., Goldenring, J.R., and Bader, D.M. (2006). CytLEK1 is a regulator of plasma membrane recycling through its interaction with SNAP-25. Mol. Biol. Cell 17, 3176–3186.

Rebola, N., Lujan, R., Cunha, R.A., and Mulle, C. (2008). Adenosine A2A receptors are essential for long-term potentiation of NMDA-EPSCs at hippocampal mossy fiber synapses. Neuron 57, 121–134.

Rehm, H., Wiedenmann, B., and Betz, H. (1986). Molecular characterization of synaptophysin, a major calcium-binding protein of the synaptic vesicle membrane. EMBO J. 5, 535–541.

Ren, Z., Riley, N.J., Garcia, E.P., Sanders, J.M., Swanson, G.T., and Marshall, J. (2003). Multiple trafficking signals regulate kainate receptor KA2 subunit surface expression. J. Neurosci. 23, 6608–6616.

Rivera, R., Rozas, J.L., and Lerma, J. (2007). PKC-dependent autoregulation of membrane kainate receptors. EMBO J. 26, 4359–4367.

Rossetto, O., Seveso, M., Caccin, P., Schiavo, G., and Montecucco, C. (2001). Tetanus and botulinum neurotoxins: turning bad guys into good by research. Toxicon 39, 27–41.

Saka, Y., Hagemann, A.I., Piepenburg, O., and Smith, J.C. (2007). Nuclear accumulation of Smad complexes occurs only after the midblastula transition in Xenopus. Development 134, 4209–4218.

Saka, Y., Hagemann, A.I., and Smith, J.C. (2008). Visualizing protein interactions by bimolecular fluorescence complementation in *Xenopus*. Methods 45, 192–195.

Sampedro, M.N., Bussineau, C.M., and Cotman, C.W. (1981). Postsynaptic density antigens: preparation and characterization of an antiserum against postsynaptic densities. J. Cell Biol. 90, 675–686.

Schiavo, G., Santucci, A., Dasgupta, B.R., Mehta, P.P., Jontes, J., Benfenati, F., Wilson, M.C., and Montecucco, C. (1993). Botulinum neurotoxins serotypes A and E cleave SNAP-25 at distinct COOH-terminal peptide bonds. FEBS Lett. 335, 99–103.

Schiavo, G., Matteoli, M., and Montecucco, C. (2000). Neurotoxins affecting neuroexocytosis. Physiol. Rev. 80, 717–766.

Selak, S., Paternain, A.V., Fritzler, M.J., and Lerma, J. (2006). Human autoantibodies against early endosome antigen-1 enhance excitatory synaptic transmission. Neuroscience 143, 953–964.

Söllner, T., Whiteheart, S.W., Brunner, M., Erdjument-Bromage, H., Geromanos, S., Tempst, P., and Rothman, J.E. (1993). SNAP receptors implicated in vesicle targeting and fusion. Nature 362, 318–324.

Song, I., and Huganir, R.L. (2002). Regulation of AMPA receptors during synaptic plasticity. Trends Neurosci. 25, 578–588.

Sorkin, A. (2004). Cargo recognition during clathrin-mediated endocytosis: a team effort. Curr. Opin. Cell Biol. 16, 392–399.

Staudinger, J., Lu, J., and Olson, E.N. (1997). Specific interaction of the PDZ domain protein PICK1 with the COOH terminus of protein kinase C-alpha. J. Biol. Chem. 272, 32019–32024.

Sun, W., Yan, Q., Vida, T.A., and Bean, A.J. (2003). Hrs regulates early endosome fusion by inhibiting formation of an endosomal SNARE complex. J. Cell Biol. 162, 125–137.

Tao-Cheng, J.H., Du, J., and McBain, C.J. (2000). Snap-25 is polarized to axons and abundant along the axolemma: an immunogold study of intact neurons. J. Neurocytol. 29, 67–77.

Terashima, A., Cotton, L., Dev, K.K., Meyer, G., Zaman, S., Duprat, F., Henley, J.M., Collingridge, G.L., and Isaac, J.T. (2004). Regulation of synaptic strength and AMPA receptor subunit composition by PICK1. J. Neurosci. 24, 5381–5390.

Wiedenmann, B., and Franke, W.W. (1985). Identification and localization of synaptophysin, an integral membrane glycoprotein of Mr 38,000 characteristic of presynaptic vesicles. Cell 41, 1017–1028.

Xia, J., Zhang, X., Staudinger, J., and Huganir, R.L. (1999). Clustering of AMPA receptors by the synaptic PDZ domain-containing protein PICK1. Neuron 22, 179–187.

Xue, Y., Zhou, F., Zhu, M., Ahmed, K., Chen, G., and Yao, X. (2005). GPS: a comprehensive www server for phosphorylation sites prediction. Nucleic Acids Res. 33, W184–W187.

Yan, Q., Sun, W., McNew, J.A., Vida, T.A., and Bean, A.J. (2004). Ca2+ and N-ethylmaleimide-sensitive factor differentially regulate disassembly of SNARE complexes on early endosomes. J. Biol. Chem. 279, 18270–18276.

Yang, B., Gonzalez, L., Jr., Prekeris, R., Steegmaier, M., Advani, R.J., and Scheller, R.H. (1999). SNARE interactions are not selective. Implications for membrane fusion specificity. J. Biol. Chem. 274, 5649–5653.